Transactions, SMiRT-24
BEXCO, Busan, Korea - August 20-25, 2017
Division VI

EXPERIMENTAL AND NUMERICAL STUDIES OF COMBINED IN-PLANE AND OUT-OF-PLANE BEHAVIOR OF SC WALL PIERS

Brian Terranova[1], Andrew Whittaker[2], Nebojsa Orbovic[3]

[1] Research Engineer, University at Buffalo, 232 Ketter Hall, Buffalo, New York, 14260, USA
[2] Professor and MCEER Director, Department of Civil, Structural, and Environmental Engineering, University at Buffalo, 212 Ketter Hall, Buffalo, New York, 14260, USA
[3] Technical Specialist, Canadian Nuclear Safety Commission, Canada

ABSTRACT

Steel-plate concrete (SC) composite shear walls are composed of steel faceplates, infill concrete, shear studs bonding the faceplate to the infill, and tie rods linking the faceplates. To date, a significant amount of studies have focused on the in-plane (IP) response of SC walls, but the effect of out-of-plane (OOP) loading on the IP response has not been rigorously addressed.

Three medium-scale rectangular SC wall specimens were built and tested under force-controlled monotonic OOP loading and displacement-controlled cyclic IP loading. The magnitude of OOP load and its effects on IP capacity, and the effect of tie rod spacing were the focus of this experimental investigation. The aspect ratio of all walls was 0.6. The height, length, and width of the SC wall piers were 36, 60, and 12 inches, respectively. The test matrix, test setup, and key results of the experiments (i.e., cyclic IP behavior, peak loads and drifts, and damage to the specimens) are presented. A maximum tie rod spacing of one-half the wall thickness is recommended for SC walls when OOP demands are expected to crack the infill concrete.

The physical tests were simulated using the general-purpose finite element program LS-DYNA. Numerical models validated for the prediction of the IP response of SC wall piers were utilized as a starting point for this study. The numerical simulations are presented and compared with the experimental results to formally validate the numerical model for combined IP and OOP loading. The numerical model predicts well IP cyclic response when OOP demands do not damage the infill concrete.

INTRODUCTION

Steel-plate concrete (SC) composite walls consisting of steel faceplates, infill concrete, and connectors used to anchor the steel faceplates together to the infill concrete may be a viable construction alternative to reinforced concrete (RC) and steel plate shear walls. The use of steel faceplates by-and-large eliminates the need for formwork, and the plates serve as primary reinforcement for in-plane (IP) loading. The challenges associated with SC walls include joining the shells in the field, field inspection of the concrete behind the faceplates, and the interaction of co-existing IP and out-of-plane (OOP) loadings that has not yet been adequately characterized.

The IP behavior of SC walls has been studied extensively, numerically and experimentally, by Varma and his co-workers (e.g., Seo et al. (2016) and Varma et al. (2013)), Epackachi et al. (2014, 2015), and others. However, there is limited information on the OOP behavior of SC walls. Yang et al. (2016) executed three full-scale experiments investigating the OOP cyclic behavior of SC walls. The parameters considered in that study were shear span-to-depth ratio and steel faceplate thickness, where the shear span-to-depth ratio for OOP loading is defined as the vertical distance between the line of OOP loading and the base of the wall divided by the wall thickness.

Bhardwaj et al. (2015) investigated the effects of OOP forces on the IP capacity of SC walls using numerical tools developed in LS-DYNA (LSTC, 2013) by Kurt et al. (2013) for IP behavior. The results

of a limited number of numerical simulations indicated that the shear span-to-depth ratio and the magnitude of the OOP load significantly affect the IP capacity of SC wall piers. Terranova et al. (2017) also conducted a numerical study to investigate the effect of OOP loading on the IP response of SC walls. The key design variables considered in that study were aspect ratio, reinforcement ratio, axial load, shear span-to-depth ratio for OOP loading, and magnitude of the OOP load.

The research published to date on the behavior of SC walls under combined IP and OOP loadings is limited. Herein, the results of three medium-scale rectangular SC wall specimens built and tested under force-controlled monotonic OOP loading and displacement-controlled cyclic IP loading at the Bowen Laboratory at Purdue University are presented. The magnitude of OOP load and its effects on the IP capacity of SC walls was the focus of this experimental investigation; the effects of tie bar spacing were also investigated. The test matrix, test setup, and key results of the experiments (i.e., cyclic IP behavior, peak loads and drifts, and damage to the specimens) are presented in the next section.

The physical tests were simulated using the general-purpose finite element program LS-DYNA. Numerical models developed by Epackachi et al. (2014, 2015), validated for the prediction of the IP response of SC wall piers, were utilized as a starting point for this study. The numerical simulations are presented and compared with the experimental results to formally validate the numerical model for combined IP and OOP loading. The limitations of the numerical model are also discussed.

PHYSICAL TESTING OF SC WALL PIERS

This section of the paper presents details and results of the physical tests on the SC wall piers conducted at Purdue University. The test matrix, test fixture, and results of the experiments are presented in the subsections.

Test Matrix and Test Fixture

The matrix of tests is presented in Table 1, wherein f_c' is concrete compressive strength and A_c is the plan area of the infill concrete. The specimens were labelled CNSC1, CNSC2 and CNSC3. Each specimen was 12 in. thick, which includes the two 3/16-inch steel faceplates. The resultant faceplate reinforcement ratio (total area of faceplates divided by total area of wall) is 0.031, which is significant by comparison with reinforced concrete shear walls. The faceplates were constructed with ASTM Grade A36 steel, with minimum specified yield strength of 36 ksi and minimum specified tensile strength of 58 ksi. Based on tension coupon tests, the yield strength and tensile strength of the steel faceplate material were 47 ksi and 80 ksi, respectively. Each specimen had an aspect (height-to-length) ratio of 0.6.

Table 1: CNSC test matrix

Specimen	Height (in.)	Length (in.)	Tie spacing (in.)	Stud spacing (in.)	Target out-of-plane force
CNSC1	36	60	12	3	$2\sqrt{f_c'}A_c$
CNSC2	36	60	6	3	Cracking
CNSC3	36	60	12	3	Cracking

The shear studs and tie bars were fabricated from carbon steel with nominal yield and ultimate stress of 50 and 75 ksi, respectively. The 3/8-inch diameter tie bars were spaced at a distance equal to the wall thickness (=12 in.) in CNSC1 and CNSC3, and one-half the wall thickness (=6 in.) in CNSC2. The spacing of the shear studs (connectors) is presented in Table 1. The faceplate slenderness ratio ($=s_s/t_p$, where s_s is the spacing of the connectors [shear studs and cross ties], and t_p is the faceplate thickness) was 16 for CNSC1, CNSC2 and CNSC3, noting that the limiting value specified in Supplement No. 1 to AISC N690s1 (AISC, 2015) for steel with yield strength of 36 ksi is 28. Each wall was founded on a large re-usable foundation designed and constructed by Purdue University. The connection of the foundation to

the wall was designed to develop the capacity of the faceplates, with the goal of forcing inelastic action into the walls above the foundation.

The last column in Table 1 identifies the target out-of-plane (OOP) force to be imposed prior to in-plane loading. The amplitude of the out-of-plane (OOP) loadings for CNSC1, CNSC2 and CNSC3 were tied to equations derived in the early 1960s for shear resistance of plain concrete beams reinforced for flexure only. The concrete contribution to shear strength of $2\sqrt{f_c'}A_c$ is traditionally used for reinforced concrete design in the United States, although it has limited technical basis. This empirical equation is unconservative for low longitudinal reinforcement ratios and conservative for high reinforcement ratios: for shallow specimens subjected to monotonic loading to failure in the absence of co-existing in-plane loadings. The effect of section depth (= wall thickness in this case), for which an increase in depth results in a decrease in shear strength of plain concrete, could not be investigated given the specimen dimensions studied here. Cracking denotes imposing an OOP loading sufficient to introduce a diagonal crack in the concrete. The OOP loading was imposed statically and not cycled during the IP loading to failure.

A photograph of the test fixture and a 3D rendering of the fixture are shown in Figure 1a and 1b, respectively. The OOP setup consisted of one 660-kip dual action actuator and beams to apply the OOP load to the specimen. The OOP load was applied 18 inches above the foundation, and the resulting ratio of shear span-to-depth was 1.5. In-plane loading was imposed on the specimen via loading beams and two 660-kip dual action actuators. The actuator clevises were detailed to accommodate the rotations associated with the IP and OOP loadings.

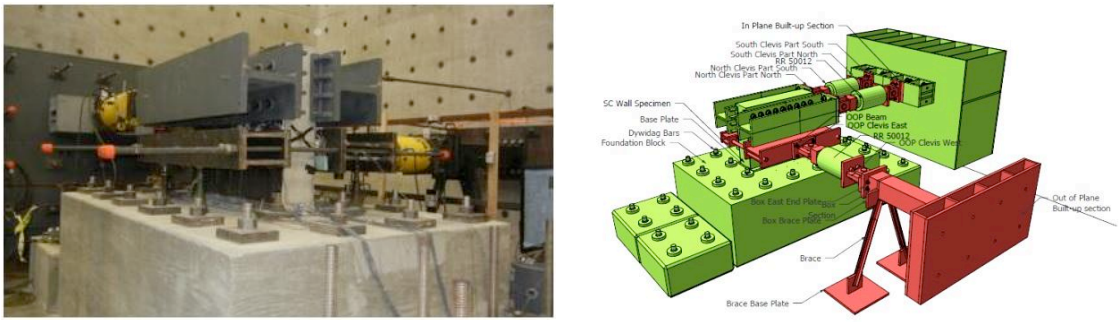

(a) photograph of the text fixture b) 3D rendering of the test fixture

Figure 1: CNSC test setup (courtesy of Purdue University)

CNSC Experiments

The concrete compressive strength of CNSC1, CNSC2, and CNSC3 on the day of testing were 7700 psi, 5300 psi, and 5300 psi, respectively, as determined by cylinder breaks. CNSC1 was initially subjected to four cycles of OOP loading, at magnitudes of 30, 60, 90, and 120 kips, respectively. The OOP load was then maintained at a constant value of 120 kips ($=1.96\sqrt{f_c'}A_c$)[1] and incremental cyclic IP loading imposed. The cycles are fully reversed loading, namely, one cycle is a push half cycle followed by a pull half cycle. CNSC2 was initially subjected to five cycles of OOP loading, at magnitudes of 30, 60, 90, 120 and 240 kips, respectively, to crack the wall due to OOP shear. Cracking of the specimen due to OOP load was first observed at 220 kips. The OOP load was then maintained at 240 kips ($=4.73\sqrt{f_c'}A_c = 1.2*(2\sqrt{f_c'}A_c + A_s f_y d/s)$, where f_c' is concrete compressive strength, A_c is plan area of infill concrete, A_s, f_y, and s are the area, tensile yield strength, and spacing of the shear reinforcement, respectively, and d is the effective depth of the cross section) and then incremental cyclic IP loading was

[1] The concrete area is the product of the length of the pier (60 in.) and the thickness of the concrete (11.625 in.).

imposed. CNSC3 was subjected to five cycles of OOP loading, at magnitudes of 50, 100, 150, 200 and 250 kips, respectively, to crack the infill concrete due to OOP shear. The OOP load was then maintained at 250 kips ($=4.92\sqrt{f_c'}A_c$) and incremental cyclic IP loading imposed. Stressing of the OOP loading beams to the specimen cracked the concrete prior to testing.

The IP load-displacement relationship and backbone curves for CNSC1, CNSC2, and CNSC3 are presented in Figures 2a, 2b, and 2c, respectively. Points A, B, C, and D in the figures represent the onset of concrete cracking caused by the IP load, yielding of steel faceplates, buckling of steel faceplates, and concrete crushing, respectively. The tests were terminated at the displacement × shown on the plots. A tie bar on the north end of the wall ruptured in cycle 13 during testing of CNSC2; the approximate point of its rupture is identified in Figure 2b by point E. Concrete cracking at the open ends of the wall under IP loading, steel faceplate yielding, steel face plate buckling, and concrete crushing of CNSC1 (CNSC2) [CNSC3] occurred at drift ratios of 0.23% (0.15%) [0.09%], 0.38% (0.37%) [0.19%], 0.70% (0.76%) [0.50%], and 1.0% (1.14%) [0.56%], respectively, and these points were identified by visual inspection (i.e., cracking and crushing of concrete, faceplate buckling) and review of strain gage data (faceplate yielding). The termination of the experiments was governed by cyclic yielding and buckling of the steel faceplates, and spalling of the infill concrete.

Key results for CNSC1, CNSC2, and CNSC3 are presented in Table 2. The initial stiffness of the SC walls, calculated at a drift ratio less than 0.02%, is presented in the second column for the push and pull directions. The values of load and drift ratio at the onset of steel plate yielding are presented in columns three and four. The fifth and sixth column present the load and drift ratio at the onset of steel faceplate buckling. The peak loads and their corresponding drift ratios for the push and pull directions are presented in columns seven and eight. The maximum drift ratios for the experiment and their corresponding loads in the push and pull directions are presented in columns nine and ten. Note that the maximum drift ratios do not correspond to failure of the wall piers.

The peak resistances of CNSC1, CNSC2 and CNSC3 were 735 kips, 629 kips, and 504 kips, respectively. The greater strength of CNSC1 can be attributed in part to a) higher compressive strength (7700 psi versus 5300 psi) for the infill concrete, and b) a relatively low OOP shear stress. A comparison of the peak resistance of CNSC2 and CNSC3 makes clear the importance to IP strength of limiting damage due to OOP shear forces, which can be accomplished in part by the provision of closely spaced cross ties. The only meaningful difference between CNSC2 and CNSC3 was tie bar spacing because the compressive strength of the infill concrete was the same in both specimens and the maximum OOP shear stress was very similar: $4.73\sqrt{f_c'}$ for CNSC2 and $4.92\sqrt{f_c'}$ for CNSC3. In this instance, the provision of closely spaced tie bars (at $d/2$) enabled a much greater peak IP resistance (629 versus 504 kips).

The accumulated damage to the south faces of SC wall piers CNSC1, CNSC2, and CNSC3 after the final cycle are presented in Figures 3a, 3c, and 3e, respectively. The accumulated damage to the north faces are presented in Figures 3b, 3d, and 3f, respectively.

SIMULATION OF CNSC EXPERIMENTS

A model of the CNSC experiments was prepared in LS-DYNA and is presented in Figure 4; the model is composed of infill concrete, baseplate, steel faceplates, tie bars, and shear studs. The foundation was not included in the model: the bottom nodes of the baseplate were fixed. The numerical model was validated for IP response using the results of cyclic tests of IP behavior of four medium-scale rectangular SC walls by Epackachi et al. (2014, 2015). Beam, shell, and solid elements were used to model connectors, steel faceplates, and infill concrete, respectively. The Winfrith concrete model (MAT085) was used for the

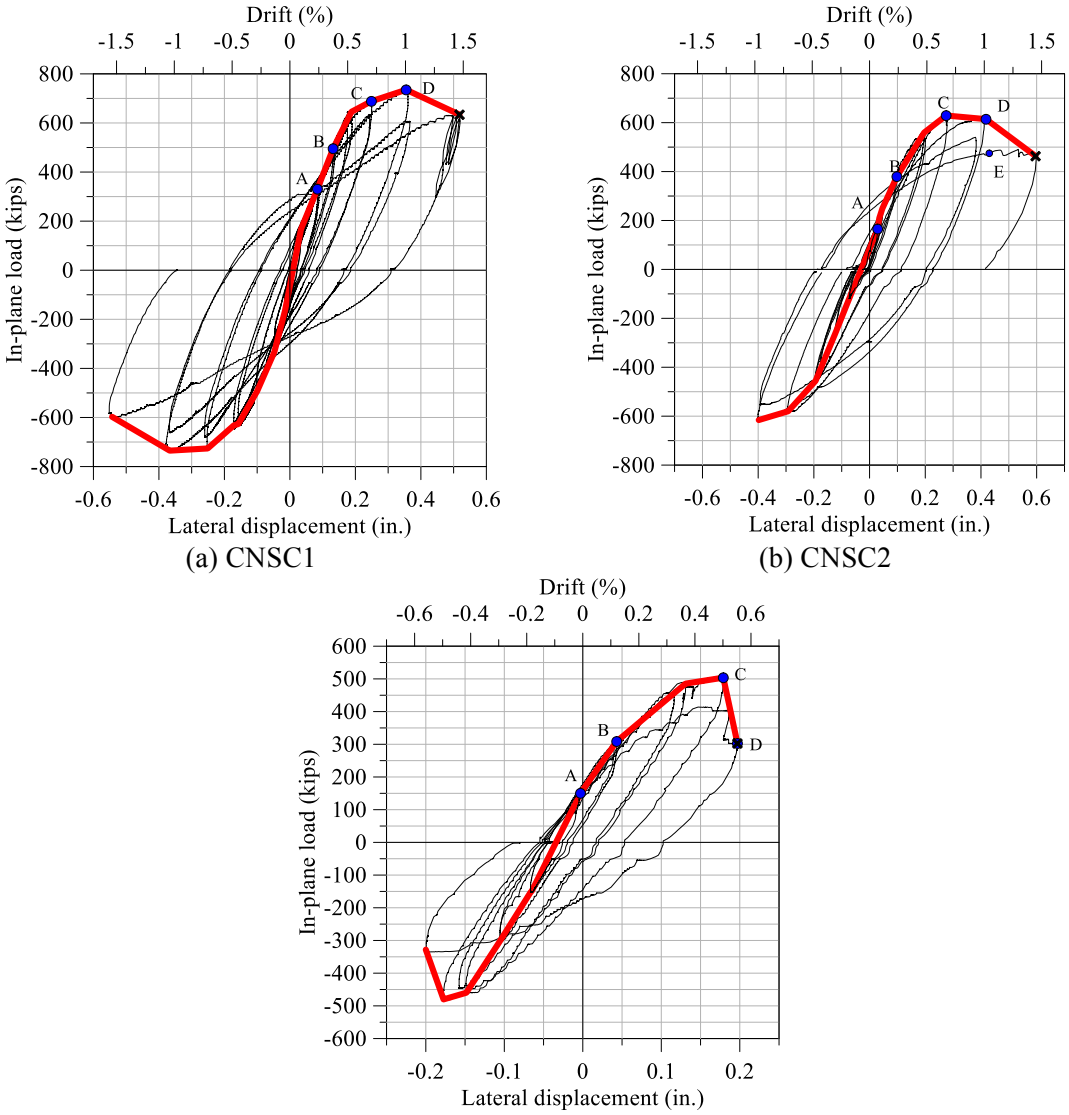

Figure 2: In-plane force-displacement relationships and backbone curves

Table 2: Summary results for CNSC experiments

	Initial stiffness (kip/in.)	Onset of steel plate yielding		Onset of steel plate buckling		Peak load		Maximum drift	
Test	Push/Pull	Load (kips)	Drift (%)	Load (kips)	Drift (%)	Load (kips) Push/Pull	Drift (%) Push/Pull	Load (kips) Push/Pull	Drift (%) Push/Pull
CNSC1	5139/4966	493	0.38	689	0.70	735/735	0.99/1.01	634/597	1.44/1.51
CNSC2	2658/3051	380	0.37	629	0.76	629/616	0.76/1.11	464/616	1.70/1.11
CNSC3	3500/3576	309	0.19	504	0.50	504/481	0.50/0.49	303/328	0.56/0.56

(a) South face, CNSC1

(b) North face, CNSC1

(c) South face, CNSC2

(d) North face, CNSC2

(e) South face, CNSC3

(f) North face, CNSC2

Figure 3: Accumulated damage to SC wall piers after final cycle for CNSC1, CNSC2 and CNSC3 (courtesy of Purdue University)

infill concrete. The OOP loading was simulated by applying nodal forces to the steel and concrete elements at a height of 18 inches above the base of the wall. Once the wall was cycled OOP and the desired OOP load was reached, the OOP load was held constant, and the wall was then subjected to displacement-controlled cyclic IP loading at its top. The follow subsections present results of the LS-DYNA simulations and these results are compared with the experiments to validate the numerical models for combined IP and OOP loading.

Simulation of CNSC1

The OOP force-displacement relationship of the SC panel for the experiment and the simulation are shown in Figure 5a. The stiffness of the SC panel in the numerical model is slightly greater than that observed in the experiment because the foundation (and its flexibility) was not modeled. The IP force-displacement relationship of the SC panel for the simulation and the experiment are shown in Figure 5b. The predictions of peak shear resistance, post-peak strength reductions, and rate of reloading/unloading stiffness for peak and post-peak IP strength cycles compared favourably with the test results; the initial IP stiffness of the numerical model is significantly larger than that of the experiment because the flexibility of the foundation was not considered in the numerical model. Figure 6 presents the observed and simulated local damage to CNSC1; cracking of the concrete and local buckling of the steel faceplates at the toes of the wall were observed in both the experiment and the numerical simulation. The numerical model cannot predict the crushing (spalling) of infill concrete observed in the experiment.

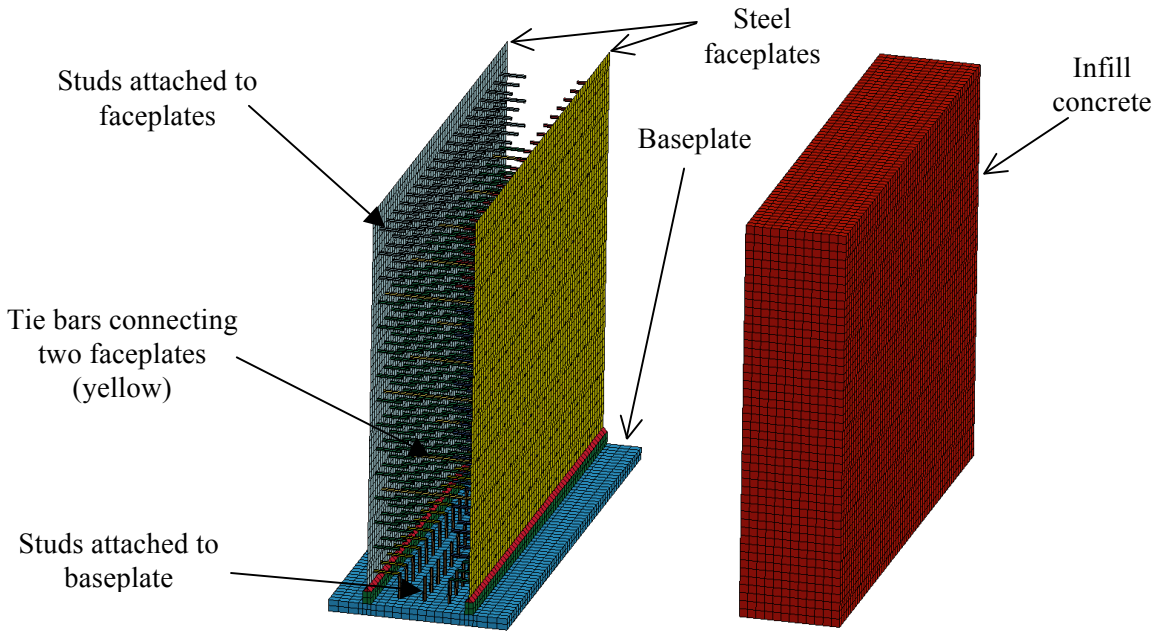

Figure 4: LS-DYNA model of the CNSC experiments

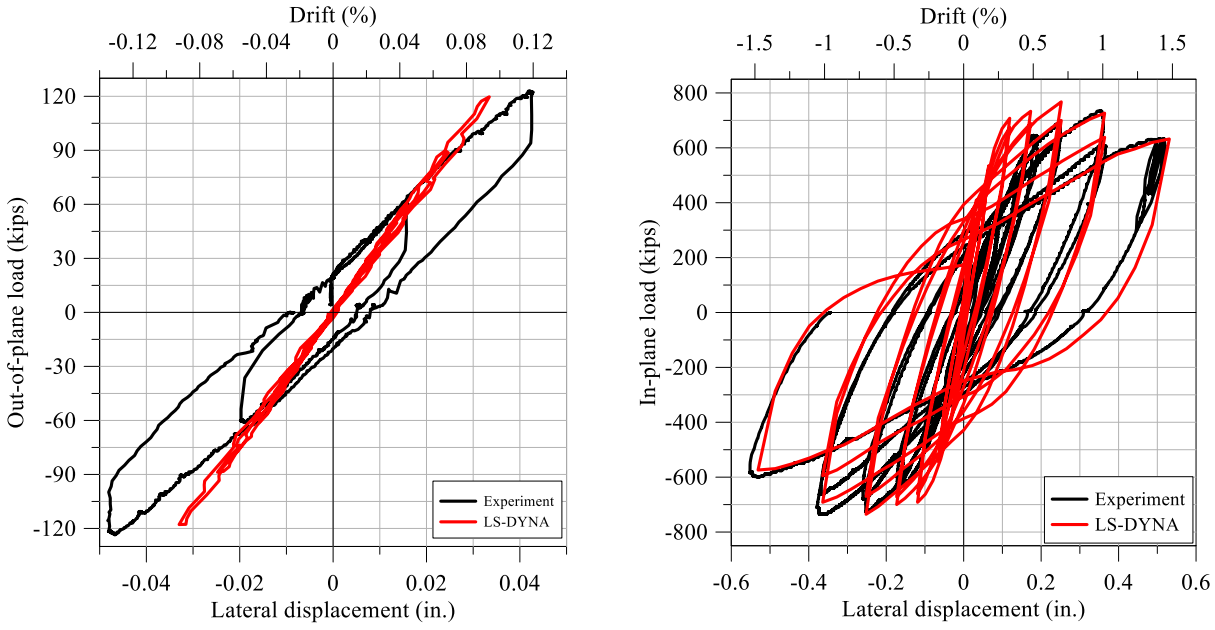

(a) Out-of-plane (b) In-plane

Figure 5: Force-displacement relationship, LS-DYNA and experiment, CNSC1

Simulation of CNSC2

Figure 7a presents the OOP force-displacement relationship for the experiment and the simulation. The stiffness of the numerical model is in relatively good agreement with that of the experiment. The IP force-displacement relationship for the simulation and the experiment are presented in 7b. The numerical model predicted the peak shear resistance and rates of reloading/unloading with reasonable accuracy. The measured and predicted damage to CNSC2 are shown in Figure 8. Local buckling of the steel faceplates

and cracking of the concrete are seen in both the experiment and the simulation. Large concrete strains are predicted and crushing of concrete was observed at the toes of the wall.

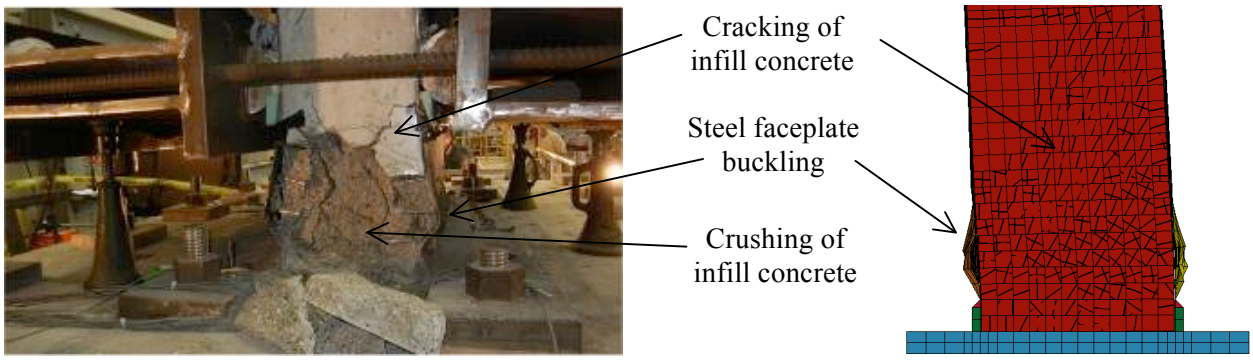

Figure 6: Observed and predicted damage to CNSC1

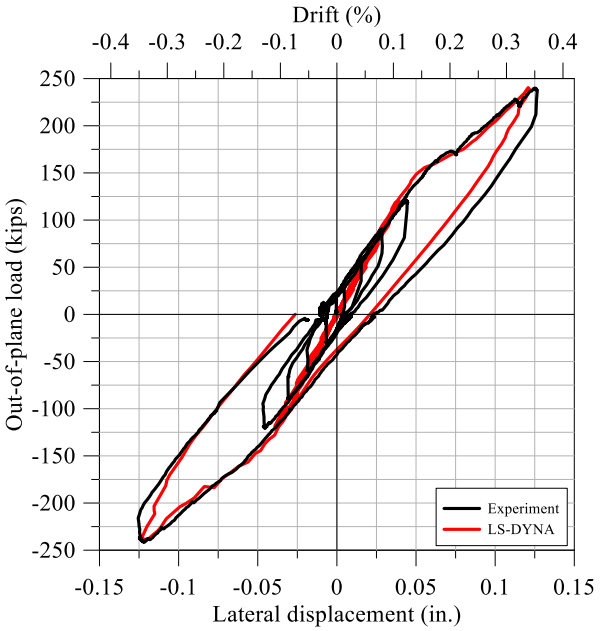

(a) Out-of-plane

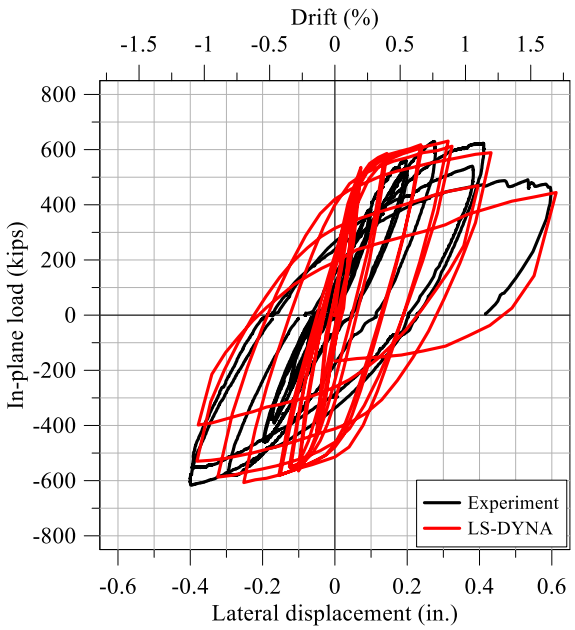

(b) In-plane

Figure 7: Force-displacement relationships, LS-DYNA and experiment, CNSC2

Simulation of CNSC3

The OOP force-displacement relationship for the experiment and numerical model are presented in Figure 9a. Similar to the simulation of CNSC1, the numerical model is slightly stiffer for OOP loading than that measured in the experiment. The simulated and measured IP force-displacement relationships for CNSC3 are presented in Figure 9b; the numerical model over predicted the peak IP capacity by 12% and did not predict the loss of IP capacity observed in the experiment. In the experiment, significant buckling of the steel faceplate at the Northeast corner of the wall and spalling of the infill concrete triggered the failure of CNSC3. The damage to the infill concrete was not predicted using the Winfrith concrete model, which assumes elastic-perfectly plastic behaviour in compression. The numerical model predicted buckling of the East steel faceplate and concrete cracking on the North and South faces (seen in Figure 10). The Winfrith model enabled the development of large compressive strains in the infill concrete, but not

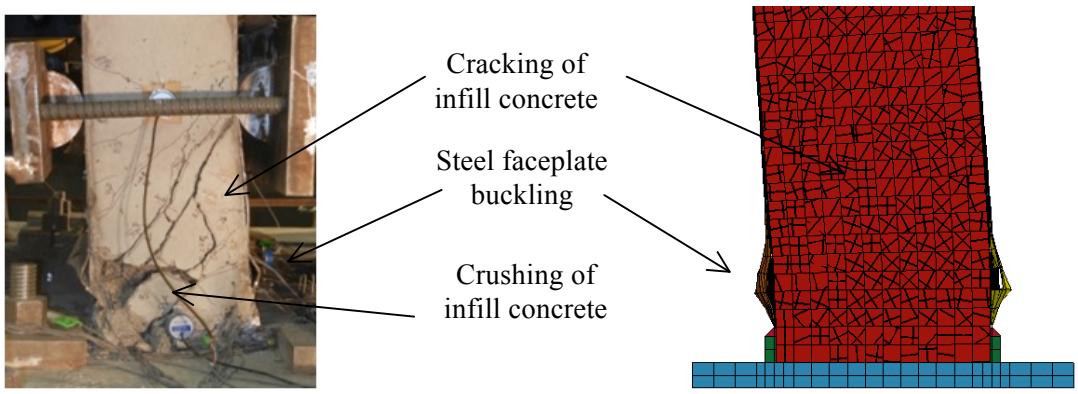

Figure 8: Observed and predicted damage to CNSC2

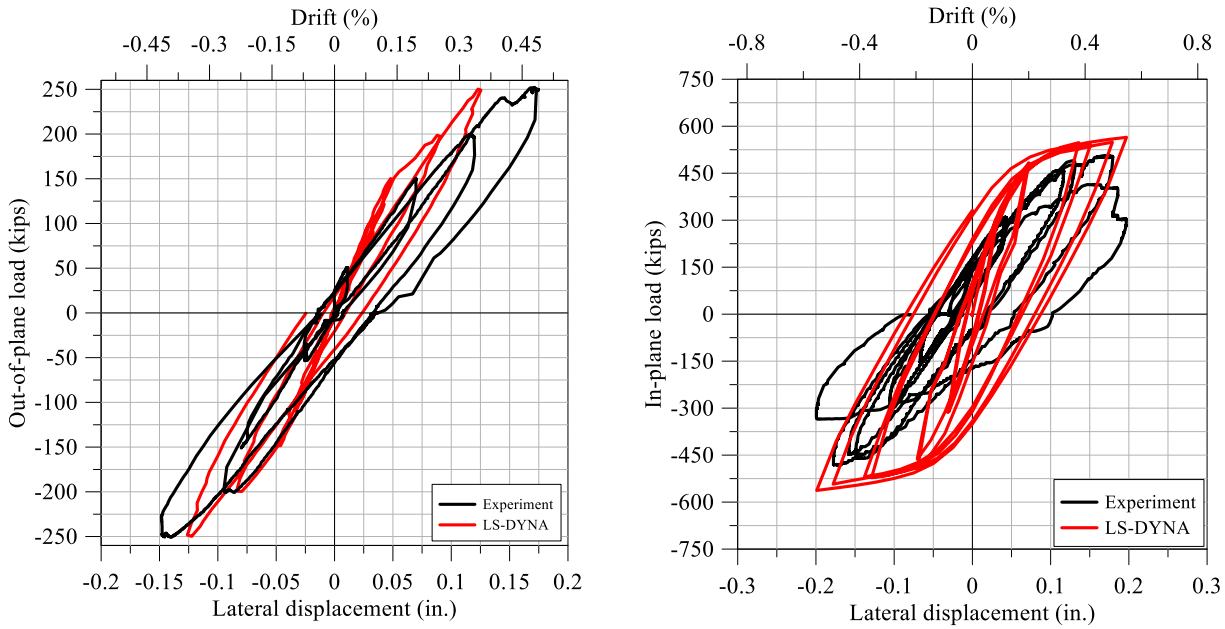

(a) Out-of-plane (b) In-plane

Figure 9: Force-displacement relationships, LS-DYNA and experiment, CNSC3

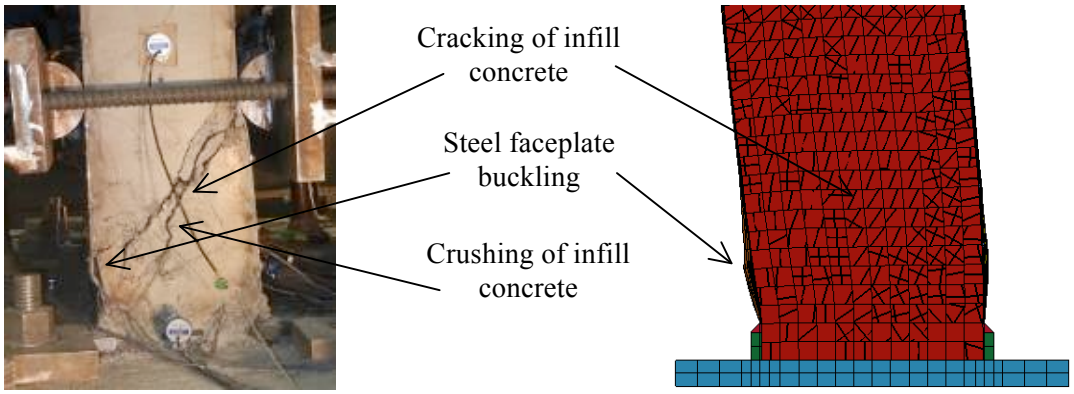

Figure 10: Observed and predicted damage to CNSC3

damage in the form of spalling, for which erosion strains (a numerical workaround) would have to be specified. A new material model would be needed to capture this loss of strength at large compressive strains.

CONCLUSIONS

Three medium-scale rectangular SC wall specimens were built and tested under force-controlled monotonic OOP loading and displacement-control cyclic IP loading. The results of the experiments indicate that the OOP load has a significant effect on the IP behavior of SC composite shear walls; the effects become very significant as the applied OOP load develops an average shear stress that is greater than the inclined cracking load of the concrete. Significant improvement in IP response was observed using a tie bar spacing equal to half of the wall thickness for SC walls subjected to larger OOP loads sufficient enough to cause inclined cracking of the concrete. A maximum tie rod spacing of one-half the wall thickness is recommended for SC walls when OOP demands are expected to crack the infill concrete.

The three experiments were simulated using the general-purpose finite element program LS-DYNA. The predictions of the numerical models of the tested wall piers were compared with cyclic force-displacement relationships (IP and OOP) and observed damage (i.e., cracking of the infill concrete and buckling of the steel faceplates). The numerical model predicts well IP cyclic response when OOP demands do not damage the infill concrete. The predictions of response for CNSC1 (low OOP shear stress) were very good, reasonable for CNSC2 (high OOP shear stress but tie bars at spacing $d / 2$) and somewhat poor for CNSC3 (high OOP shear stress and tie bars at spacing d). One reason for the poorer predictions for CNSC2 and CNSC3 can be traced to the use of the Winfrith model, which assumes elastic perfectly plastic behavior in compression.

ACKNOWLEDGEMENTS

The CNSC funded much of the work described in this paper, including the execution of the experiments in the Bowen Laboratory at Purdue University. Much of the test fixture design and construction, and the specimen construction and testing, were performed under the leadership of Professor Amit Varma at Purdue University. Purdue graduate student Mr. Saahas Bhardwaj worked closely with Professor Varma on the experimental tasks. We acknowledge the financial support of CNSC and thank Professor Varma and Mr. Saahas Bhardwaj for their critical contributions to the test program.

REFERENCES

American Institute of Steel Construction (AISC). (2015). "Specification for safety-related steel structures for nuclear facilities including supplement no. 1," *ANSI/AISC N690s1-15*, Chicago, IL.

Bhardwaj, S. R., Kurt, E. G., Terranova, B., Varma, A. H., Whittaker, A. S., and Orbovic, N. (2015). "Preliminary investigation of the effects of out-of-plane loading on the in-plane behavior of SC walls," *Transactions, 23rd Conference on Structural Mechanics in Reactor Technology*, Manchester, UK.

Epackachi, S., Nguyen, N., Kurt, E., Whittaker, A. S. and Varma, A. H. (2014). "In-plane behavior of rectangular steel-plate composite shear walls," *Journal of Structural Engineering*, 141, 1-9.

Epackachi, S., Whittaker, A. S., Varma, A. H., and Kurt, E. (2015). "Finite element modeling of steel-plate concrete composite wall piers," *Engineering Structures*, 100, 369-384.

Livermore Software Technology Corporation (LSTC). (2013). *LS-DYNA keyword user's manual*, V 971, Livermore, CA.

Seo, J., Varma, A. H., Sener, K. C. and Ayhan, D. (2016). "Steel-plate composite (SC) walls: In-plane shear behavior, database and design," *Journal of Constructional Steel Research*, 119, 202-215.

Terranova, B., Epackachi, S., and Whittaker, A. S. (2017). "Effect of out-of-plane loading on the in-plane response of SC wall piers," *Proceedings, 16th World Conference on Earthquake Engineering*, Santiago, Chile.

Yang, Y., Jingbo, L., Nie, X., and Fan, J. (2016). "Experimental research on out-of-plane cyclic behavior of steel-plate composite walls," *Journal of Earthquake and Tsunami*, 10, 1-16.

Varma, A. H., Malushte, S., Sener, K. C., and Lai, Z. (2013). "Steel-plate composite (SC) walls for safety related nuclear facilities: design for in-plane force and out-of-plane moments," *Nuclear Engineering and Design*, 269, 240-249.